Master's Thesis of Science
in Agricultural Biotechnology

Characterization and application of bacteriophage CSA13 and its endolysin LysCSA13 as biocontrol agents targeting *Staphylococcus aureus*

황색포도상구균 저감화를 위한 박테리오파지 CSA13과 이로부터 분리된 엔돌라이신 LysCSA13의 특성 분석 및 생물방제제 활용에 관한 연구

February, 2019

The Graduate School
Seoul National University
Department of Agricultural Biotechnology

Yo Yeon Cha

ABSTRACT

Staphylococcus aureus is one of the notable human pathogens which can be easily encountered in dietary and clinical surroundings. Furthermore, it is known to form biofilm by sessile communities encased in an extracellular matrix, during various food processing procedures. Biofilms possess specific advantages over planktonic cells, as they are highly resistant to the conventional antibiotics and other environmental stress. For this reason, staphylococcal biofilms are recognized as a significant problem in the food industry and the use of bacteriophage or endolysin has been regarded as a promising alternative for antibiotics. In the current study, bacteriophage CSA13 was isolated from chicken, and subsequently, its morphology, physiology, and genomics were characterized. This *Podoviridae* phage displayed extended host inhibition effect of up to 23 hours of persistence. Its broad host spectrum included MSSA, MRSA, local *S. aureus* isolates as well as non-aureus staphylococci strains. Moreover, phage CSA13 could successfully remove over 78% and 93% of MSSA and MRSA biofilms, respectively. Genomic analysis revealed 17,034 bp-long genome containing predicted 18 ORFs without tRNAs, representing the typical structure of staphylococcal *Podoviridae* family. Among 18 genes, a putative endolysin gene, which was highly homologous to *N*-acetyl-muramoyl-L-alanine

amidase, was identified. LysCSA13, an endolysin of CSA13, consists of an N-terminal CHAP (cysteine, histidine-dependent amidohydrolases /endopeptidases) domain as an enzymatic active domain and a C-terminal SH3 domain as a cell wall binding domain. LysCSA13 showed strong antimicrobial activity against all tested 15 staphylococcal strains. In addition, high efficacy of LysCSA13 to remove staphylococcal biofilm was observed on various surfaces including polystyrene, glass and stainless steel, displaying approximately 80-90% decrease in biofilm mass. Furthermore, LysCSA13 effectively removed staphylococcal sessile cell formed on stainless steel and glass by 1-3 log units compared with the untreated control. Scanning electron microscopy analysis visualized the effective deformation and removal of cells embedded in the biofilm matrix. The results indicate that LysCSA13 can effectively control staphylococcal planktonic cell as well as biofilms regardless of contact surface matrix and suggest the possible use of LysCSA13 as a promising bio-control agent in various food processing environment.

Keywords: *Staphylococcus aureus,* Bacteriophage, Endolysin, Biofilm

Student Number: 2017-23691

CONTENTS

Ⅰ. INTRODUCTION

Biofilm formation is one of the major concerns in the food industry as the ability of bacteria to adhere to food-contact surfaces poses a risk to human health by providing a reservoir of contamination for pathogens (Gutierrez et al. 2016). Staphylococci, including *S. aureus,* are known to form biofilms on various biomaterials and can persist in clinical and food settings, gaining high resistance to action of typical antimicrobial agents, harsh environmental conditions, and host immunity (Li and Lee 2017). Indeed, antibiotic therapies are generally unsuccessful for the treatment of biofilm-associated infections, mainly due to the low permeability of antibiotics to the biofilm matrix and the presence of a large number of persister cells with poor metabolic activity (Flemming and Wingender 2010, Lewis 2008, Stewart 2002). Therefore, development of novel anti-biofilm strategies has been urgently required.

Bacteriophage-encoded endolysins have been the focus of research as alternative antimicrobials since they have several advantages over conventional antibiotics such as potent species-specific activities and low probability for developing bacterial resistance. Furthermore, endolysins can destabilize the biofilm structure as well as kill replicating and non-replicating

bacteria embedded in the biofilm matrix and thereby disrupt the biofilm (Dunne et al. , Sharma et al. 2018). Disruption of staphylococcal biofilms by endolysin has been reported in previous studies with *S. aureus* endolysins, LysH5 and LysK (Fenton et al. 2013, Gutierrez et al. 2014). Endolysin from a *Podoviridae S. aureus* bacteriophage have been first attempted using endolysin SAL-2 (Son J. S. et al. 2010b).

While these studies have focused on biofilms formed only on the surface of polystyrene, stainless steel and glass are also commonly used in the food processing environment. In addition to polystyrene, stainless steel and glass can be contaminated by food pathogens interacting with the surface, initiating cellular growth, and consequently leading to biofilm formation (Marques et al. 2007). This study proposed the use of endolysin LysCSA13 to reduce staphylococcal biofilm on the various food contact surfaces including polystyrene, stainless steel and glass.

In this study, virulent bacteriophage CSA13 (accession no. MH107118) infecting *S. aureus* was isolated from whole raw chicken sample, and its characteristics in terms of physiology, genomics, and bioinformatics were investigated. Moreover, we identified a putative endolysin gene, *LysCSA13*, in the genome of CSA13 phage. This endolysin gene was cloned and expressed in *Escherichia coli*, and the purified

endolysin was biochemically characterized. The biofilm reduction efficacy of LysCSA13 was evaluated on various food contact surfaces including polystyrene, stainless steel and glass for its potential as a bio-control agent.

Ⅱ. MATERIALS AND METHODS

2.1. Bacterial strains, media and growth conditions

The bacterial strains used in this study are summarized in Table 1. All the bacterial strains were grown in tryptic soy broth (TSB) medium (Difco, Detroit, MI) at 37℃ with aeration. *Escherichia coli* DH5α and BL21 (DE3) were grown in Luria-Bertani (LB) broth (Difco) at 37 ℃ and used in the cloning and expression of proteins, respectively.

2.2. Phage isolation and propagation

Influent water from Guri-si sewage treatment facility (Gyeongi,-do, South Korea), raw chicken and ducks were used to screen bacteriophages using *S. aureus* strains as host. Influent water was centrifuged at 10,000 × *g* for 5 min and filtered to remove bacterial cells. In the case of raw chicken and duck samples, they were homogenized for 1 min with 1 L of Bolton broth supplemented with Bolton Broth Selective Supplement (10 mg Cefoperazone, 10 mg Trimethoprim, 10 mg Vancomycin, and 25 mg Cyclohexamide). The sample was then incubated at 42 ℃ for 12 h in micro-aerobic condition (6% O_2, 10% CO_2, 84% N_2). After incubation, the aforementioned broth was centrifuged at 10,000 × *g* for 5 min and filtered to

remove bacterial cells. After treatment of samples, 5 mL of the filtered sample was mixed with 5 mL of 2X Tryptic soy broth (TSB) and sub-cultured with the host strains at 37 °C, 220 rpm for 12 h. After incubation, the culture was centrifuged at 10,000 × *g* for 10 min and filtered to exclude any bacterial cells.

For phage propagation, TSB was first sub-inoculated with the host *S. aureus* strain and incubated at 37 °C, 220 rpm for 1.5 h. Subsequently, the phage was added at multiplicity of infection (MOI) of 1, followed by 3 h incubation in the same condition. To prepare phage in a high-titer, the propagated phages were precipitated with polyethylene glycol (PEG) 6000 and condensed using CsCl density gradient ultracentrifugation (Chang et al. 2013). Finally, to confirm the phage plaque formation, the supernatant was overlaid on soft agar (TSB containing 0.4% agar) with 100 μL of the host *S. aureus* strain and incubated at 37 °C, static for 12 h.

2.3. Transmission electron microscopy (TEM)

Diluted CsCl-purified bacteriophage samples in SM buffers were analyzed using transmission electron microscopy (TEM). The phage suspensions were placed on a carbon-coated copper grid and negatively stained with 2% uranyl-acetate (pH 4.0). Samples were examined under an

energy-filtering transmission electron microscope at an operating voltage of 120 kV (Kwiatek et al. 2012). Bacteriophages were identified and classified according to the guidelines of the International Committee on Taxonomy of Viruses.

2.4. Bacterial challenge assay

Fifty-milliliter of TSB was sub-inoculated with the host *S. aureus* strain, and incubated at 37 °C until the early exponential growth phase. The culture was then infected with the phage at MOI of 1. The OD_{600} was measured each hour after phage infection for 25 h and no measurement was held at time points between 14^{th} to 22^{nd} h. (Park M. et al. 2012). An un-infected culture was used as a control. All the experiments were performed in triplicate.

2.5. Bacteriophage host range

The bacterial strains listed in Table 1 were incubated overnight at 37 °C. Each bacterial culture was added to 5 mL of soft agar (TSB containing 0.4% agar) and overlaid on TSA plates. Subsequently, 10 µL of the diluted lysates containing isolated phages were applied onto the prepared plate and incubated at 37 °C for at least 6 h to obtain single

plaques. After incubation, we could determine the infectivity based on the clarity of the spots. One of the bacteriophages which showed most wide host range was selected for further studies

2.6. Receptor analysis of phage CSA13

S. aureus RN4220, a strain free of prophages, restriction mechanisms and capsules (Wann et al. 2006), was used in this study (Table 1). To identify the phage receptor, we constructed Δ*tagO*/RN4220 mutant, which lacks the peptidoglycan-anchored wall teichoic acid (WTA) (Swoboda et al. 2010), and its complementary strain using plasmid pRB474-*tagO*, which was constructed by sub-cloning the *tagO* gene into an *Escherichia coli-S. aureus* shuttle expression vector (Brückner 1992). We carried out spotting assay with the wild type RN4220, Δ*tagO*/RN4220 mutant and the *tagO* complementary strain.

2.7. One-step growth curve assay of phage CSA13

One-step growth curve analysis was performed as previously described (Lu et al. 2003). Briefly, phage was mixed with the host *S. aureus* strain in its early exponential growth phase at MOI of 0.001. After 10 min of incubation at 25 °C for adsorption, it was centrifuged at 6,000

× *g* for 10 min. The pellet containing infected cells was suspended in 50 mL of fresh TSB and incubated at 37 °C, 220 rpm. Two sets of samples were collected every 5 min for up to 1 h. To release the intracellular phages, $CHCl_3$ was added to one of them, and the eclipse period was determined. Subsequently, titer of each sample was immediately assessed by the double-layer agar plate method, and latent period, eclipse period and burst size were analyzed. All the experiments were performed in triplicate.

2.7. Biofilm reduction assay of phage CSA13

Biofilm reduction assay was performed based on a previous study with some modifications (Kelly et al. 2012). Two different *S. aureus* strains, *S. aureus* Newman and *S. aureus* CCARM 3793, incubated in TSB supplemented with 0.25% D-(+)-glucose (TSBg) were prepared. Afterwards, 1:100 dilutions were performed by adding 2 μL of a pure cell suspension to 198 μL of TSBg in each well of 96-well polystyrene plate, while 200 μL of TSBg was added as a negative control. After incubating the microplate for 24 h at 37 ˚C, all wells were washed for three times with phosphate buffered saline (PBS). Once the biofilm was formed, it was treated with 200 μL of phage lysate (10^9 – 10^{11} PFU/mL) in SM buffer or a

buffer-only negative control. After incubation at 37 ˚C, static, for 24 h, phage lysate was removed and each well was washed for once with PBS and stained with 1% crystal violet. Additional washing with PBS was done, followed by solubilizing with 33% acetic acid. The absorbance of the obtained solution was measured at 570 nm and the sessile biomass was presented as A_{570} value.

2.7. Bacteriophage genomic DNA purification of phage CSA13

Bacteriophage genomic DNA was purified as previously described (Wilcox et al. 1996). Prior to purification, the phage lysates were treated with DNase and RNaseA at 37 °C for 1 h to remove bacterial nucleic acid contaminants. The phage lysates were then treated with lysis buffer containing 0.5 M of EDTA, 10 mg/mL of proteinase K and 1% of sodium dodecyl sulfate (SDS) for 1 h at 56 °C. Finally, ethanol precipitation was performed, followed by phenol-chloroform DNA purification.

2.8. Full-genome sequencing and bioinformatics analysis of phage CSA13

The sequence of purified CSA13 phage genomic DNA was analyzed with Genome Sequencer FLX titanium system (Roche,

Mannheim, Germany) and assembled with the GS de novo assembler software (Roche) at Sanigen Inc., South Korea. Open reading frames (ORFs) were predicted using the FGENESB (http://www.softberry.com), Glimmer v3.02 (Delcher et al. 2007) and GeneMarkS (Besemer et al. 2001) software packages. The ORFs were annotated using InterProScan (Žiedaitė et al. 2005) and BLASTP (Altschul et al. 1997) programs. Sequence alignment of CSA13 and staphylococcal phages from *Podoviridae*, *Myoviridae*, *Siphoviridae* families was performed by ClustalW (Thompson et al. 1994), using DNA sequence of the whole genome. Complete genome sequence of each taxon was acquired from the NCBI (www.ncbi.nlm.nih.gov) database. Sequence relationships were inferred using the Neighbor-joining method (Saitou and Nei 1987), and the phylogenetic tree was constructed using MEGA7.0.21 (Kumar et al. 2016). The bootstrap value derived from 5,000 replicates was considered to represent the evolutionary history of the analyzed taxa (Felsenstein 1985). The evolutionary distances were computed using the p-distance method (Nei and Kumar 2000). Comparative genome analysis of CSA13 and other *Podoviridae* phages was conducted by progressiveMauve (Darling Aaron C.E. et al. 2004, Darling Aaron E. et al. 2010) and ACT (Artemis Comparison Tool) (Carver et al. 2005). The minimum score cutoff value

of ACT analysis was 20. The complete genome sequence of *S. aureus* phage CSA13 was deposited in GenBank under accession number MH107118.

2.9. Bioinformatics analysis of LysCSA13

From the complete genome sequence of the *S. aureus* phage CSA13, a gene (phCSA13_007) encoding the LysCSA13 endolysin was identified. The domain architecture of LysCSA13 was analyzed using InterProScan program (https://www.ebi.ac.uk/interpro). The amino acid sequences of several staphylococcal endolysins harboring the CHAP domain and SH3_5 domain were aligned using BLAST (Altschul et al. 1997) or Clustal X2 (Larkin et al. 2007).

2.9. Cloning and purification of LysCSA13

The endolysin gene (phCSA13_007) was PCR amplified using the primers LysCSA13F and LysCSA13R. The resulting PCR product was subcloned into pET28a (Novagen, Madison, WI), which harbors an N-terminal hexahistidine (6 x His)-tag sequence. For LysCSA13 endolysin expression, *E. coli* BL21 (DE3) cells were transformed with the resulting

plasmid. Protein expression was induced by the addition of 0.5 mM isopropyl-β-thiogalactopyranoside (IPTG, final concentration) upon reaching an OD_{600} of 0.7, after which cells were further incubated at 18 °C for 20 h. Cells were suspended in lysis buffer (50 mM sodium phosphate, 300 mM NaCl, pH 8.0) and lysed by sonication (Branson Ultrasonics, Danbury, CT). The clarified supernatant containing soluble proteins was obtained by centrifugation at 15,000 × g for 30 min, followed by filtration (0.22-μm pore size; Millipore). Recombinant protein was purified using a Ni-nitrilotriacetic acid (NTA) Superflow column (Qiagen Gmbh, Germany) according to the manufacturer's instructions. The identity and purity of the protein were confirmed by sodium dodecyl sulfate polyacrylamide gel electrophoresis (SDS-PAGE) (Dunne et al. 2014). Purified protein was exchanged into storage buffer (50 mM sodium phosphate, 300 mM NaCl, 30% glycerol, pH 8.0) using a PD Miditrap G-25 (GE Healthcare, Amersham, Bucks, UK) and stored at −80 °C until use.

2.9. Characterization of the LysCSA13 endolysin

The lytic activity of LysCSA13 was assessed by the turbidity reduction assay (Son Bokyung et al. 2012). Briefly, exponentially growing cells (*S. aureus* RN4220) were harvested and suspended in reaction buffer

(20 mM Tris-HCl, pH 8.0) to an OD_{600} of approximately 1.0 (Gaeng et al. 2000). After the addition of purified endolysin (30 nM–300 nM), the OD_{600} values were periodically monitored (0, 10, 20, 30, 40, 50, and 60 min). For Gram-negative bacteria, exponentially growing cells were pretreated with a buffer containing 20 mM Tris-HCl (pH 8.0) and 100 mM ethylenediaminetetraacetic acid (EDTA) for 5 min at 25 °C. The cells were washed three times with reaction buffer to remove residual EDTA prior to the endolysin addition.

To test the susceptibility of cells to LysCSA13 in various pHs, 300 nM of LysSA11 was added to *S. aureus* RN4220 cell suspensions in the following buffers: 20 mM sodium acetate for pH 4.3-5.0; 20 mM Tris-HCl for pH 6.5-8.0; 20 mM Glyine for pH 9.0; and 20 mM Sodium carbonate for pH 10.0. To assess the effect of temperature on LysCSA13 enzymatic activity, endolysins incubated at different temperatures (20–75 °C) were used in the turbidity reduction assay. The influence of NaCl on the lysis activity was evaluated by using different NaCl concentrations (0– 100 mM) (Son Bokyung et al. 2012)

The effects of metal ions on lysis activity were determined as previously reported (Schmelcher et al. 2012). To chelate metal ions attached to the endolysin, EDTA (5.0 mM; final concentration) was added to the

endolysin (300 nM) and incubated at 37 °C for 1 h. The EDTA was then removed by exchanging the endolysin into 20 mM Tris-HCl buffer (pH 8.0) using a PD Miditrap G-25. The EDTA-treated enzyme was added to cell suspensions with metal ions ($CaCl_2$, $MgCl_2$, $MnCl_2$, $CuCl_2$, or $ZnCl_2$; 1.0 mM final concentration), and the lysis activity was assayed in reaction buffer.

2.9. Biofilm reduction assay on 96-well polystyrene plate

A biofilm disruption assay was performed as previously described with some modifications (Wu et al. 2003). Six different staphylococcal strain incubated in TSB medium supplemented with 0.25 % $_D$-(+)-glucose (Sigma) was prepared and was sub-cultured to the same media in a 96-well polystyrene microplate. Glucose was supplemented to the medium as it can induce the biofilm formation by inducing *ica* gene, which mediate synthesis of polysaccharide intercellular adhesion (PIA) or polymeric *N*-acetyl-glucosamine (PNAG) of biofilm (Jin et al. 2005) and most staphylococci were adhered to the plates more in glucose-rich medium than in glucose-poor medium (Moreira et al. 2013). After incubating the microplate for 24 h at 37 °C, all wells were washed with PBS. Once the biofilm was formed, the experimental group wells were filled with

LysCSA13 (50 nM-1000 nM), whereas reaction buffer (20 mM Tris-HCl, pH 8) was added to the negative control. After the incubation for 2 h at 37 °C, each well was washed once with PBS and stained with 1.0 % crystal violet. Additional washing with PBS, followed by solubilizing with 33 % acetic acid, was done. The absorbance of the obtained solution was measured at 570 nm and the sessile biomass was presented as the A_{570} value.

2.9. Biofilm reduction assay against biofilm on stainless steel and glass surfaces

Stainless steel (2 x 2 cm^2, type: No.4) coupons and glass cover slips (2 x 2 cm^2) were sterilized by dipping into 70 % ethanol and autoclaved at 121˚C, 15 min. The biofilm formation and endolysin treatment was performed as described previously (Sillankorva et al. 2008), with some modification. Briefly, stainless steel and glass coupons were placed on the wells of a 6 well microplate (Corning, New York, NY, USA), each well containing 3 ml of TSB medium supplemented with 0.25 % D-(+)-glucose (Sigma). Bacterial culture was added to each well and the microplate was incubated at 37 ˚C under static condition for 24 h. Stainless steel coupon and glass coupon with biofilm were immersed twice in PBS

and placed in new microplates. After fixation of biofilm, the plates were incubated at 37 ˚C with different concentrations (100-1000 nM) of LysCSA13. Control experiments were performed at same conditions with 3 ml of reaction buffer (20 mM Tris-HCl, pH 8). The staining and measurement of biofilm mass was performed as described above.

To determine the counts of bacteria attached to each coupon, viable cell count assay was performed following previously reported method with some modification (Gutierrez et al. 2014). Once the biofilm was developed, stainless steel and glass was scratched four times with a sterile swab and then immersed into 9 ml of PBS buffer. A vigorous shaking for 1 min allowed the disaggregation of the biofilm. Finally, several serial dilutions were plated onto Tryptic soy agar (TSA) (Difco) and incubated at 37 ˚C.

2.9. Characterization of biofilm using field emission scanning electron microscopy (FESEM)

To prepare samples for scanning electron microscopy (SEM), the procedures of the biofilm assay on stainless steel coupon in a 6-well culture plate was processed as describe above. The microscopic sample was prepared following a previously reported method (Sillankorva et al. 2008). A field-emission scanning electron microscope (SIGMA 55VP, Carl Zeiss,

United Kingdom) at national instrumentation center for environmental management (NICEM, Seoul, South Korea) was used to observe the biofilm formation.

III. RESULTS

3.1. Isolation and characterization of bacteriophages

Four bacteriophages of *S. aureus* were isolated from sewage influent, raw chicken and raw duck samples. Characteristics of each phage were summarized in Table 1. All of the isolated phage formed clear plaques against host strain. For morphological characterization of phages, TEM analysis was conducted and phages had isometric heads with different morphology of tails (Figure 1). Phage CSA5 belonged to *Myoviridae* family with nonflexible and contractile tails whereas CSA9 belonged to *Siphoviridae* family with flexible tails. Phage CSA13 and CSA24 belonged to *Podoviridae* family with short and non-contractile tail.

Table 1. Characteristics of newly isolated bacteriophages

Designation of phage	Family	Source	Host
CSA5	*Myoviridae*	Influent	*S. aureus* Livestock isolate 131
CSA9	*Siphoviridae*	Raw chicken	*S. aureus* RN4220
CSA13	*Podoviridae*	Raw chicken	*S. aureus* Clinical isolate FMB_1
CSA24	*Podoviridae*	Raw duck	*S. aureus* CCARM 3793

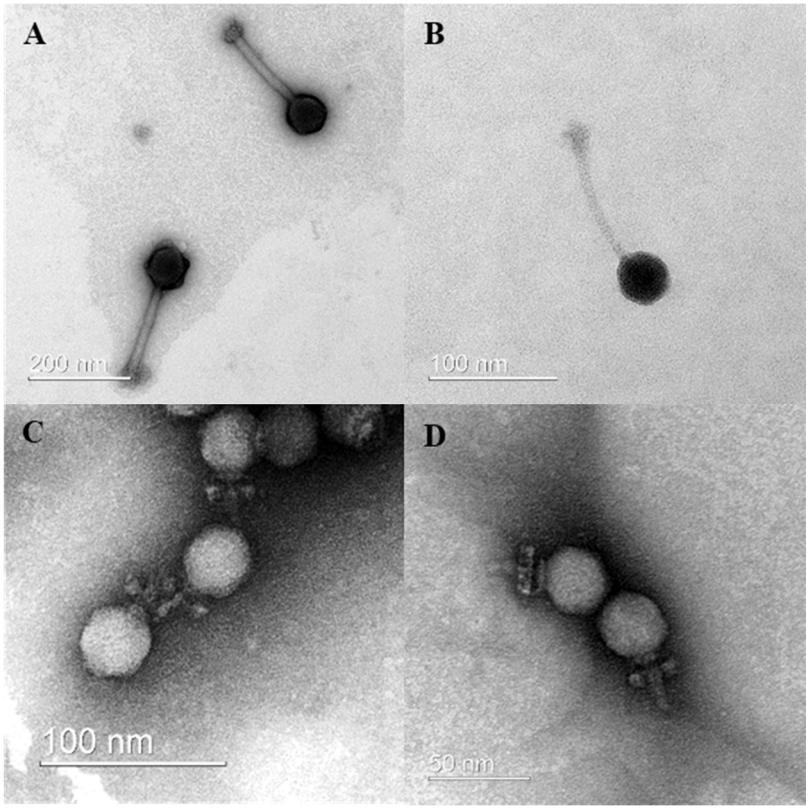

Figure 1. Transmission electron microscope of four isolated phages. Phage CSA5 (A) belongs to *Myoviridae* family, CSA9 (B) belongs to *Sipohoviridae* family, CSA13 and CSA24 belongs to *Podoviridae* family. The scale bar appeared at the bottom left corner of the image.

3.2. Bacterial challenge assay

To determine the inhibition activity of isolated bacteriophages, bacterial challenge assay was performed. The effect of four isolated phages was inoculated on each *S. aureus* host strain in early-exponential phase at MOI of 1.0. As a result, antibacterial activity for phage CSA5 and CSA24 was maintained for 14 h and 10 h, respectively (Figure 2A, C). In contrast, reduction of turbidity was observed shortly for phage CSA9 and increase of turbidity was observed due to the appearance of phage resistance cell (Figure 2B). In the case of phage CSA13, the growth inhibition of *S. aureus* persisted for up to 23 h (Figure 2D), indicating that phage CSA13 has strongest inhibitory effect among four isolated phages.

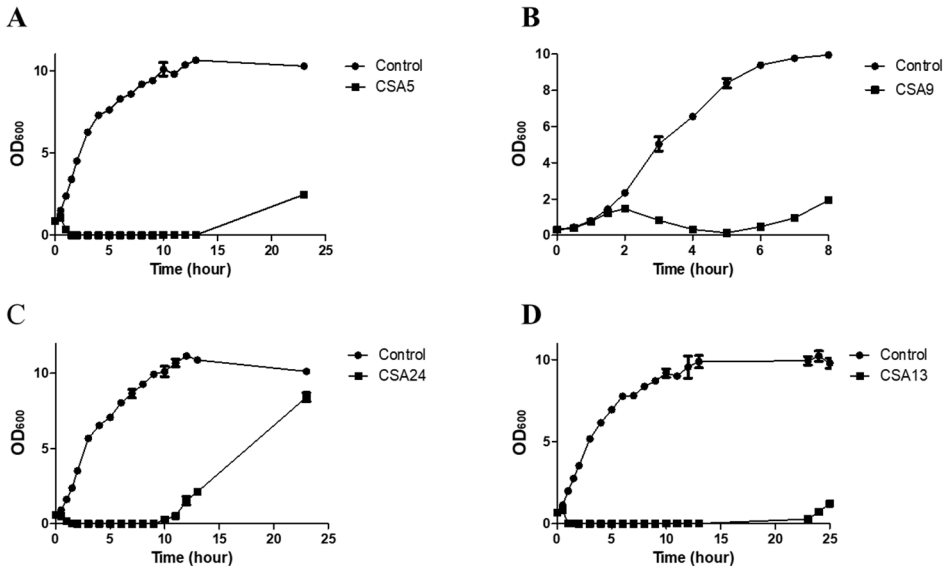

Figure 2. Bacterial challenge assay of phages against *S. aureus*. Cells were prepared in two groups; control group without phage (●) or experimental group with phages (■) with MOI of 1. The data shown are the mean values from three independent measurements and the error bars represent the standard deviations.

3.3. Host range analysis

To determine antimicrobial spectrum of four isolated phages, 28 strains of *S. aureus* including 15 isolates, 8 strains of Gram-positive, and 4 strains of Gram-negative bacteria were used as shown on Table 2. Among four isolated phages, CSA13 showed broadest host range selectively infecting *S. aureus* strains; 10 out of 12 *S. aureus* type strains including MRSA strains and all 15 *S. aureus* local isolates. In addition, phage CSA13 could infect three other staphylococcal strains other than *S. aureus* including *S. epidermis*, *S. hominis*, and *S. warneri*. As a result, phage CSA13 was chosen for further studies.

Table 2. The host range of phages

Bacterial host	CSA5	CSA9	CSA13	CSA24	Reference or source
Staphylococcal strain					
S. aureus RN4220	**T**	**C**	**T**	**-**	**(Park K. H. et al.)**
S. aureus Newman	**C**	**I**	**I**	**I**	**(Baba et al.)**
S. aureus ATCC 13301	**T**	**-**	**C**	**I**	**ATCC**
S. aureus ATCC 23235	**C**	**I**	**T**	**C**	**ATCC**
S. aureus ATCC 33586	**C**	**-**	**T**	**-**	**ATCC**
S. aureus ATCC 33593	**I**	**-**	**C**	**C**	**ATCC**
S. aureus KCTC 1916	**T**	**T**	**C**	**C**	**KCTC**
S. aureus ATCC 6538	**T**	**I**	**C**	**C**	**ATCC**
S. aureus ATCC 29213	**C**	**I**	**C**	**C**	**ATCC**
S. aureus ATCC 12600	**I**	**I**	**T**	**C**	**ATCC**
MRSA CCARM 3793	**C**	**T**	**C**	**C**	**CCARM**
MRSA CCARM 3089	**T**	**-**	**C**	**-**	**CCARM**
MRSA CCARM 3090	**T**	**-**	**I**	**I**	**CCARM**
S. haemolyticus ATCC 29970	**T**	**I**	**I**	**I**	**ATCC**
S. epidermidis ATCC 35983	**I**	**I**	**C**	**T**	**ATCC**
S. hominis ATCC 37844	**C**	**T**	**C**	**C**	**ATCC**
S. warneri ATCC 10209	**T**	**-**	**T**	**-**	**ATCC**
Other Gram-positive bacteria					
Enterococcus faecalis ATCC 29212	–	–	–	–	**ATCC**
Bacillus cereus ATCC 14579	–	–	–	–	**ATCC**
Bacillus subtilis ATCC 23857	–	–	–	–	**ATCC**
Listeria monocytogenes ATCC 19114	–	–	–	–	**ATCC**
Gram-negative bacteria					
Salmonella enterica serovar Typhimurium SL 1344	–	–	–	–	**ATCC**
Escherichia coli MG1655 ATCC	–	–	–	–	**ATCC**

47076					
Cronobacter sakazakii ATCC 29544	–	–	–	–	**ATCC**
Pseudomonas aeruginosa ATCC 27853	–	–	–	–	**ATCC**
Laboratory isolates (*S. aureus*)					
129	**T**	**T**	**C**	**-**	**Animal product**
130	**T**	**I**	**T**	**-**	**Animal product**
131	**C**	**-**	**T**	**I**	**Animal product**
134	**C**	**C**	**C**	**T**	**Animal product**
clinical isolate 0055	**C**	**T**	**C**	**T**	**Gyeongsang National University hospital**
clinical isolate 0136	**-**	**-**	**C**	**-**	**Gyeongsang National University hospital**
clinical isolate 0154	**T**	**I**	**T**	**-**	**Gyeongsang National University hospital**
clinical isolate 0212	**T**	**I**	**T**	**T**	**Gyeongsang National University hospital**
clinical isolate 0600	**C**	**I**	**C**	**T**	**Gyeongsang National University hospital**
clinical isolate FMB-1	**T**	**I**	**C**	**-**	**Cotton from hospital**
77	**T**	**T**	**T**	**-**	**Human isolate**
79	**T**	**I**	**T**	**-**	**Human isolate**
80	**T**	**I**	**C**	**-**	**Human isolate**
81	**I**	**I**	**T**	**-**	**Human isolate**
82	**T**	**I**	**T**	**-**	**Human isolate**

[a], C, clear plaque; T, turbid plaque; I, inhibition zone; -, no plaque.[b], ATCC, American Type Culture Collection; NCTC, National Collection of Type Cultures; CCARM, Culture Collection of Antimicrobial Resistant Microbes.

3.4. Receptor determination

The only known host receptor of *S. aureus* phages is peptidoglycan-anchored wall teichoic acid (WTA) (Xia et al. 2011) demonstrated that WTA is required for viral infection of *S. aureus*; thus, a *ΔtagO* mutant of *S. aureus* (RN4220*ΔtagO*) (Oku et al. 2009) was tested (Figure 3). The RN4220*ΔtagO* strain was resistant to CSA13 and the phage sensitivity was recovered by complementing the strain with *tagO* (Park Keun-Hwa et al. 2010a).

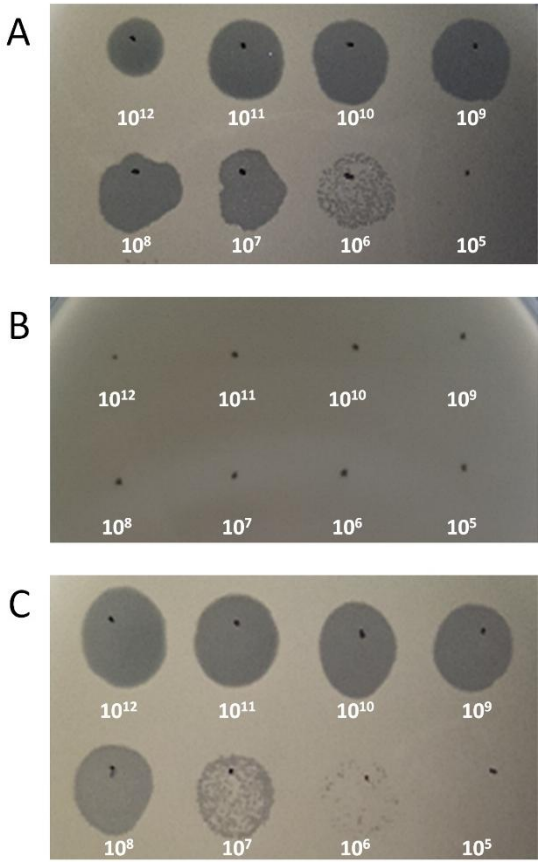

Figure 3. Wall teichoic acid (WTA)-dependent infection of S. aureus phage CSA13. Wall teichoic acid (WTA)-dependent infection of *S. aureus* phage CSA13. (**A**) Phage CSA13 lysate was spotted onto lawns of wild-type RN4220, (**B**) *ΔtagO* mutant, and (**C**) *tagO*-complemented strains. Each number indicates the titer (PFU/mL) of phage CSA13 spotted on the plate. Plaque formation indicates successful adsorption and infection by phage CSA13.

3.5. One-step growth curve assay

To determine the eclipse period, latent period, and burst size of phage CSA13, one-step growth curve analysis was conducted with the host strain. One-step growth curve is a very important index in understanding the cyclic replication pattern of phages. It was determined that the eclipse period and latent period are 15 min and 20 min, respectively. The burst size was about 230 PFU/infected cell (Figure 4).

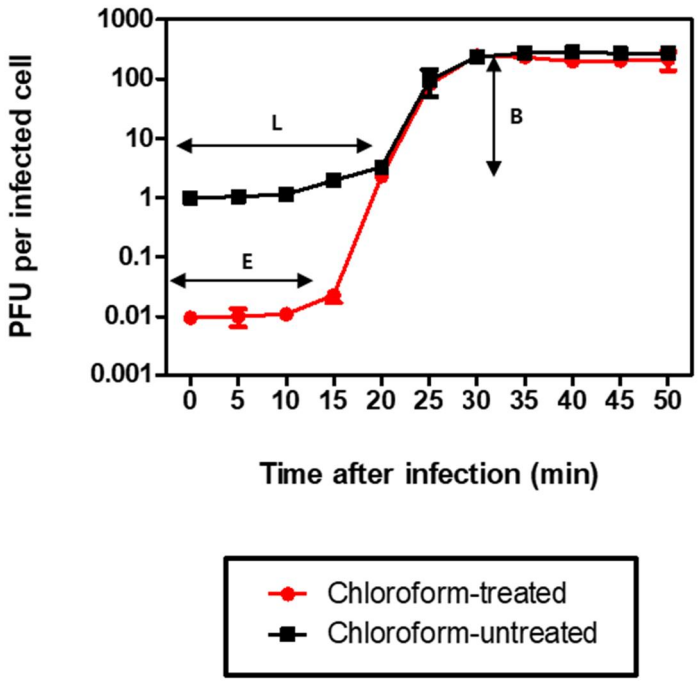

Figure 4. One-step growth curve analysis of phage CSA13. Exponential culture of *S. aureus* clinical isolate FMB-1 incubated in tryptic soy broth (TSB) medium at 37 °C, 220 rpm. Cells were prepared in two groups; chloroform treated (●) or untreated (■). E, eclipse period; L, latent period; B, burst size

3.6. Biofilm reduction assay of phage CSA13

The efficacy of phage CSA13 to reduce staphylococcal biofilm was examined by visual comparison based on crystal violet staining method. In 96-well polystyrene microplate, both *S. aureus* CCARM 3793 and Newman strains successfully formed biofilm, while *S. aureus* CCARM 3793 strain displayed about 40% stronger biofilm forming capacity than *S. aureus* Newman. Biofilms formed by both *S. aureus* CCARM 3793 and *S. aureus* Newman were successfully removed by phage CSA13 in a PFU-dependent manner. Comparing biofilm reduction efficacy of phage CSA13 against the two different strains, *S. aureus* CCARM 3793 underwent stronger anti-biofilm effect than *S. aureus* Newman. When 10^9 PFU/mL to 10^{11} PFU/mL of CSA13 was treated for 24 h, 56% to 78.5% eradication in biofilm mass was observed for *S. aureus* Newman and 86.5% to 93.4% for *S. aureus* CCARM 3793 (Figure 5). The results above correspond to lytic activity data of CSA13 (Table 2), as it formed clear plaque against *S. aureus* CCARM 3793, whereas it could only form inhibition zone against *S. aureus* Newman.

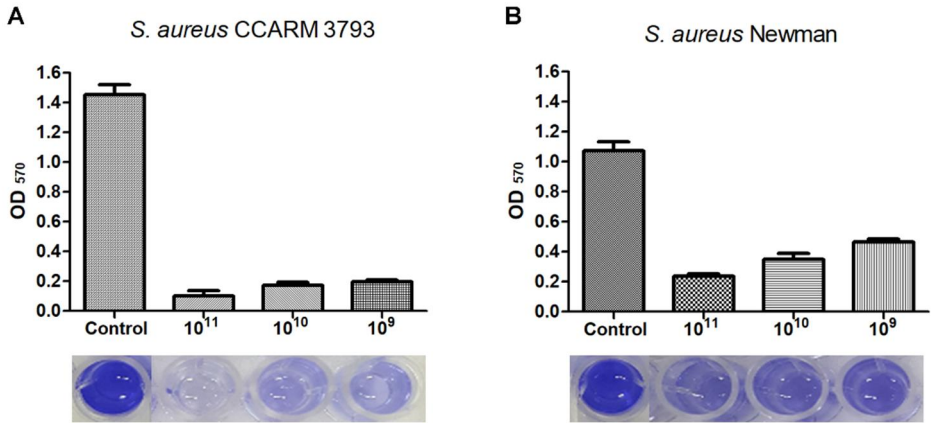

Figure 5. Removal of 24 h-old biofilm on 96-well polystyrene microplate with phage CSA13. Biofilms of CCARM 3793 (A) and *S. aureus* Newman (B) were treated with CSA13 of three different PFU for 24 h. Each column represents the mean of triplicate experiments, and error bars indicate the standard deviation.

3.6. Whole genome analysis of phage CSA13

Genomic features of phage CSA13 were revealed by whole genome sequencing. CSA13 is a double stranded DNA (dsDNA) virus with 17,034-base pair-long linear genome. The average G+C content of the genome is 28.97%, and 18 open reading frames (ORFs) but no tRNA were predicted (Figure 6). According to clusters of orthologous groups (COG) database, the ORFs were categorized into four functional groups; structure (capsid and scaffold protein, collar protein, major teichoic acid biosynthesis protein, tail fiber), lysis (N-acetylmuramoyl-L-alanine amidase, holin), DNA manipulation (DNA polymerase, ssDNA binding protein), and DNA packaging.

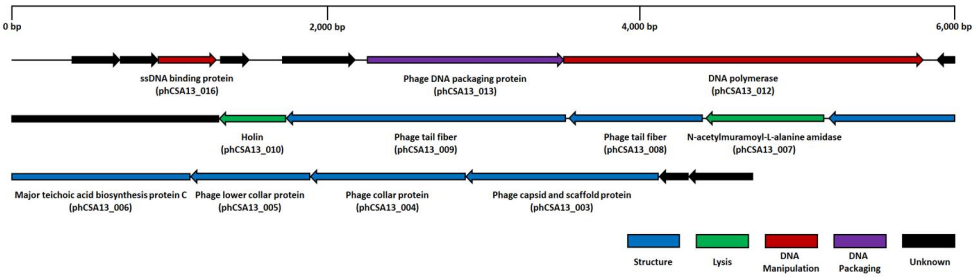

Figure 6. Genome map of phage CSA13. The arrangement of predicted ORFs on CSA13 genome. Functional groups are categorized into colors.

3.6. Comparative genome analysis of phage CSA13

Whole-genome sequence of phage CSA13 and other *S. aureus Podoviridae* phages were analyzed together with *S. aureus Myoviridae* and *Siphoviridae* phage genomes (Figure 7). From the resulting tree, *Podoviridae* phages could be differentiated from other families, while majority of *Podoviridae* phages were closely related to one another. Phage SAP-2 turned out to have highest similarity to phage CSA13, even though most *Podoviridae* phages were not as discrete as those in *Myoviridae* or *Siphoviridae* family.

In a comparison with the closest phage SAP-2, phage CSA13 exhibited strong homology (97% coverage with 97% identity) throughout the genome. As revealed in the ACT data, phCSA13_006, the structural gene coding teichoic acid biosynthesis protein C, displayed the most apparent difference against phage SAP-2 (Figure 8). In terms of amidase, the amino acid sequence comparison by protein BLAST resulted in 89% identity with the coverage of 100%.

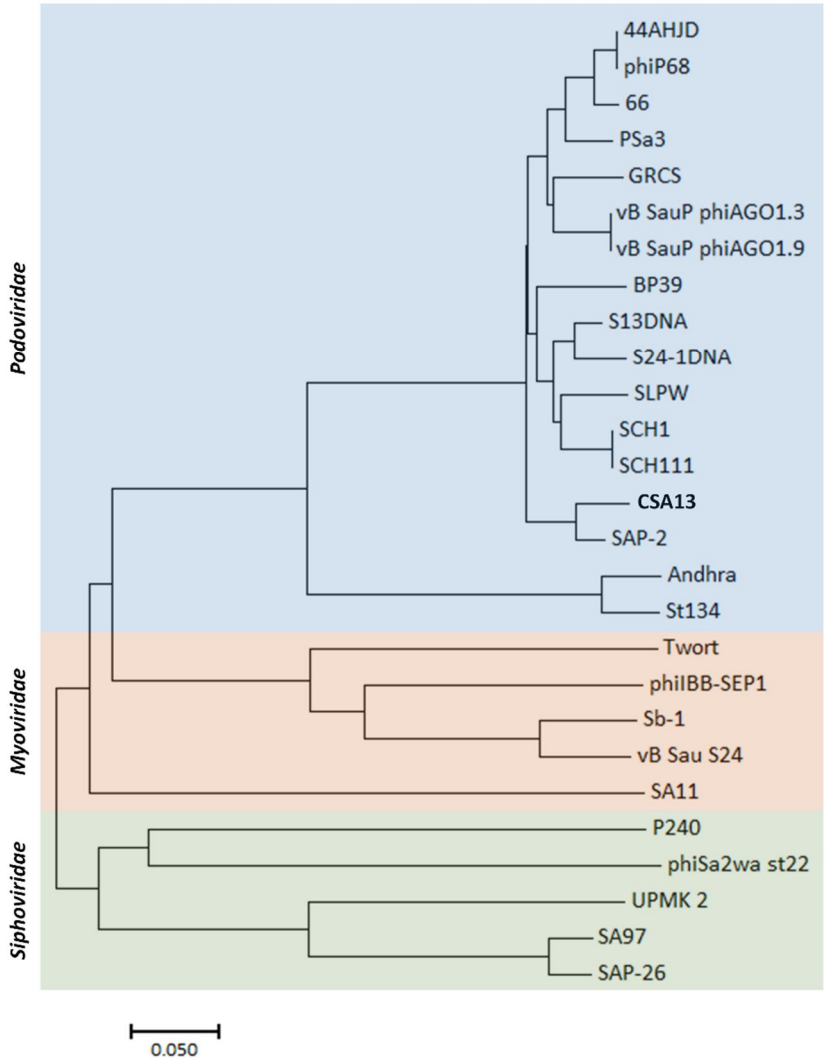

Figure 7. Phylogenetic tree of staphylococcal phages. Whole-genome sequences were aligned by ClustalW and the tree was constructed with neighbor-joining method and the evolutionary distances were computed with p-distance method by MEGA7 software.

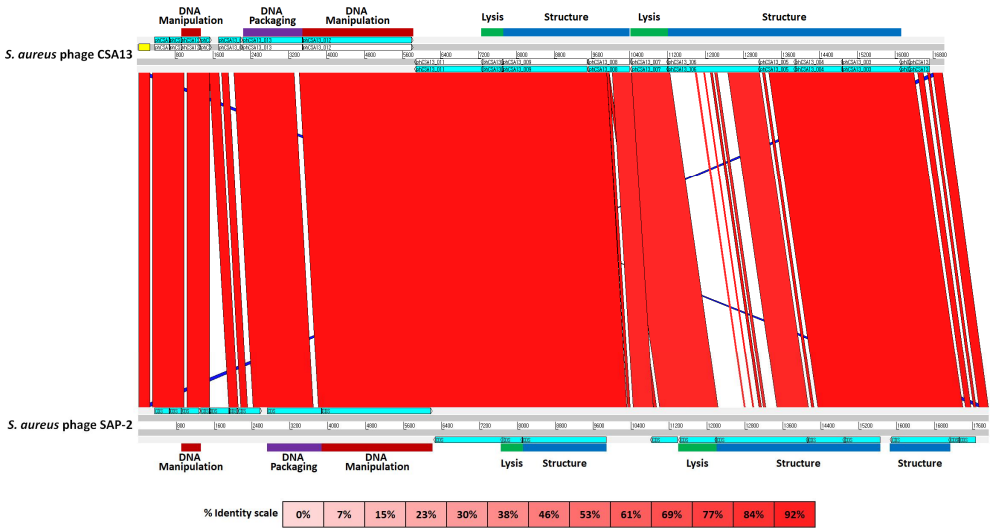

Figure 8. Comparative analysis of phage CSA13 and phage SAP-2 genomes by ACT. ORFs were designated with COG categories and corresponding color labels. The genome of phage CSA13 was annotated in an opposite direction; thus, the reverse complementary sequence was used. The color intensity of each band is proportional to the percent identity.

3.6. Identification and overexpression of LysCSA13 endolysin

From genome sequence of phage CSA13, predicted open reading frame for endolysin gene was identified and designated as *LysCSA13*. According to Pfam 28.0 analysis, LysCSA13 was predicted to be composed of CHAP domain (PF05257, E-value, 2e-11) at its N-terminus and SH3_5 domain (PF08460, E-value, 6.6e-23) at its C-terminus (Figure 9A). BLASTP analysis presented that LysCSA13 has the highest homology to an amidase from *S. aureus* phage SAP-2 (SAL-2) (YP_001491539.1, 89% identity) (Son Jee-Soo et al. 2010a) and endolysin of *S. aureus* phage phiP68 exhibited 85% homology with LysCSA13 (Figure 9B) (Vybiral et al. 2003). To date, endolysins derived from *Podoviridae* family phages are very limited and only endolysin SAL-2 was studied for its removal activity of both staphylococcal planktonic cells and biofilms. Therefore, the study of LysCSA13, the novel endolysin from *Podoviridae* family bacteriophage, will be meaningful as a potential biocontrol agent.

The LysCSA13 was cloned and overexpressed in *E. coli*. After purification, single band of the purified endolysin was observed between 26 and 34 kDa by SDS-PAGE (Figure 10A). This result was consistent with calculated molecular mass of LysCSA13 (28 kDa). The turbidity reduction assay revealed effective lytic activity of LysCSA13 against *S. aureus*

RN4220 in concentration-dependent manner. More than 70% of total cell suspension was reduced with 300 nM LysCSA13 within 10 min and even 30 nM could exert about half of its maximal lytic activity (Figure 10B).

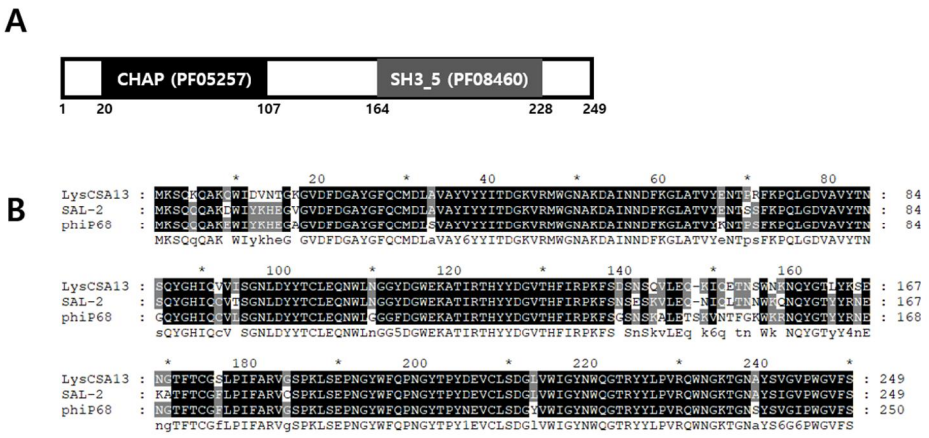

Figure 9. Modular structure of the LysCSA13 endolysin from *S. aureus* phage CSA13. (A) Schematic representation of LysCSA13. **(B)** Sequence alignment of SAL-2 endolysin. Conserved and identical residues are shaded in gray (>40% conserved) and black, respectively.

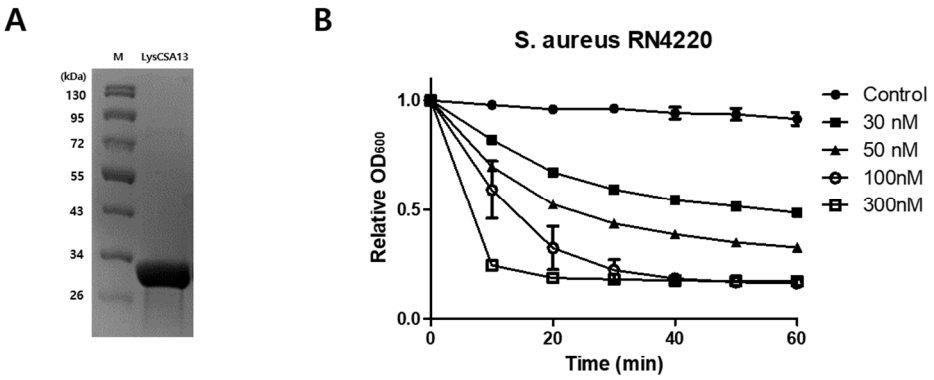

Figure 10. Purification of LysCSA13 and its lytic activity. (**A)** Purified LysCSA13 was loaded on an SDS-PAGE gel. Lane M, molecular weight marker; lane 1, purified LysCSA13 fraction. (**B)** Lysis of *S. aureus* RN4220 with four different concentrations of LysCSA13. *Black circle* negative control (no enzyme added), *Black square* 30 nM enzyme added, *black triangle* 50 nM enzyme added, *clear circle* 100 nM enzyme added, *clear square* 300 nM enzyme added. The data shown are the mean values from three independent measurements and the error bars represent the standard deviation.

3.6. Biochemical characteristic of LysCSA13

LysCSA13 was highly active at pH 7.0-9.0, with the highest activity at pH 8.0 (Figure 11A). The maximal activity of LysCSA13 was observed at 25˚C, and this endolysin could effectively lyse susceptible bacteria between 20 and 75˚C (Figure 11B). LysCSA13 exhibited a 50% reduction in lytic activity with 25 mM of NaCl, indicating this endolysin is sensitive to NaCl (Figure 11C). To study the effects of divalent ions on lytic activity of LysCSA13, the metal ions were removed from the protein using 5.0 mM EDTA. Treatment of 5.0 mM EDTA considerably decreased lytic activity of LysCSA13, demonstrating the necessities of metal ions for its full lytic activity. When 1.0 mM of Ca^{2+} or Mn^{2+} were added to the EDTA-treated endolysin, the lytic activity was fully restored. However, addition of Mg^{2+}, Zn^{2+}, and Cu^{2+} resulted in little or no recovery of activity of the EDTA-treated endolysin (Figure 11D). Taken together, LysCSA13 requires divalent metal ions, particularly Ca^{2+} or Mn^{2+} for its enzymatic activity.

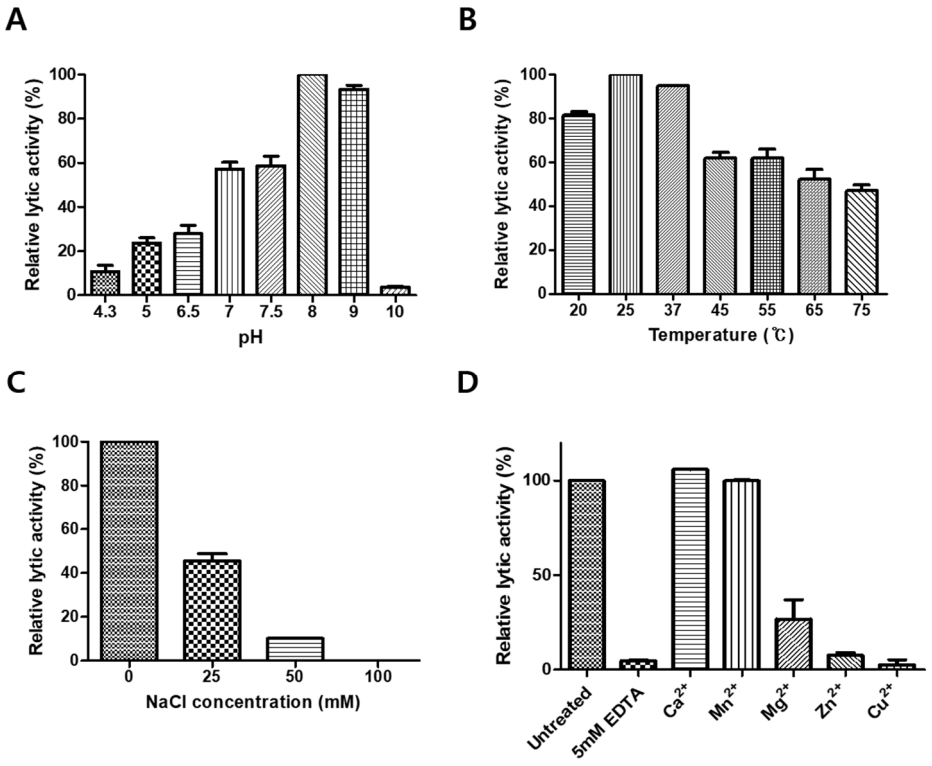

Figure 11. Biochemical characterization of LysCSA13. The effect of pH (**A**), temperature (**B**), NaCl concentration **(C)** and metal ion **(D)** on the lytic activity of LysCSA13 against *S. aureus* RN4220 cells are shown. Each column represents the mean of triplicate experiments, and error bars indicate the standard deviation.

3.6. Antimicrobial activity spectrum of LysCSA13

Antimicrobial spectrum of LysCSA13 was examined against 15 staphylococcal strain, other Gram-positive and Gram-negative bacteria (Table 3). All tested *S. aureus* strains including MRSA and 3 other staphylococcal strains such as *S. haemolyticus, S. hominis* and *S. warneri* were lysed by LysCSA13. On the other hand, this endolysin did not show the lytic activity against other Gram-positive bacteria and Gram-negative bacteria. These results indicated that LysCSA13 has a limited antimicrobial spectrum in staphylococcal species, whose peptidoglycan is cross-linked via pentaglycine interpeptide bridge (Schleifer and Kandler 1972).

Table 3. The antimicrobial spectrum of LysCSA13

Bacterial host	Lytic activity	Reference or source
Staphylococcal strain		
S. aureus RN4220	+++	(Park K. H. et al. 2010b)
S. aureus Newman	++	(Baba et al. 2008)
S. aureus ATCC 13301	+++	ATCC
S. aureus ATCC 23235	++	ATCC
S. aureus ATCC 33586	+++	ATCC
S. aureus ATCC 33593	+++	ATCC
S. aureus ATCC 6538	++	ATCC
S. aureus ATCC 29213	++	ATCC
S. aureus ATCC 12600	+++	ATCC
MRSA CCARM 3793	++	CCARM
MRSA CCARM 3089	+++	CCARM
MRSA CCARM 3090	+++	CCARM
S. haemolyticus ATCC 29970	+++	ATCC
S. hominis ATCC 37844	+++	ATCC
S. warneri ATCC 10209	++	ATCC
Other Gram-positive bacteria		
Enterococcus faecalis ATCC 29212	-	ATCC
Bacillus cereus ATCC 14579	-	ATCC
Bacillus subtilis ATCC 23857	-	ATCC
Listeria monocytogenes ATCC 19114	-	ATCC
Gram-negative bacteria		
Sarmonella enterica serovar Typhimurium SL 1344	-	ATCC
Escherichia coli MG1655 ATCC 47076	-	ATCC
Cronobacter sakazakii ATCC 29544	-	ATCC
Pseudomonas aeruginosa ATCC 27853	-	ATCC

Gram-negative bacteria were treated with EDTA. The percentage of lytic activity was obtained by turbidity reduction assay for 60 min; 1-30% +, 30-70% ++; 71-100% +++, 0% -

3.6. Biofilm reduction efficacy of LysCSA13 on the polystyrene microplate

The efficacy of LysCSA13 to reduce staphylococcal biofilm was examined using 96-well polystyrene microplate. Biofilm reduction efficacy was evaluated by visual comparison using crystal violet-staining method to confirm disruption of biofilm matrix, for two *S. aureus* strains including MRSA strains. LysCSA13 showed similar extent of biofilm reduction efficacy for two strains tested and exhibited the saturated activity at 300 nM (Figure 12). This results suggest high biofilm reduction efficacy of LysCSA13 towards staphylococcal biofilm formed on polystyrene surface.

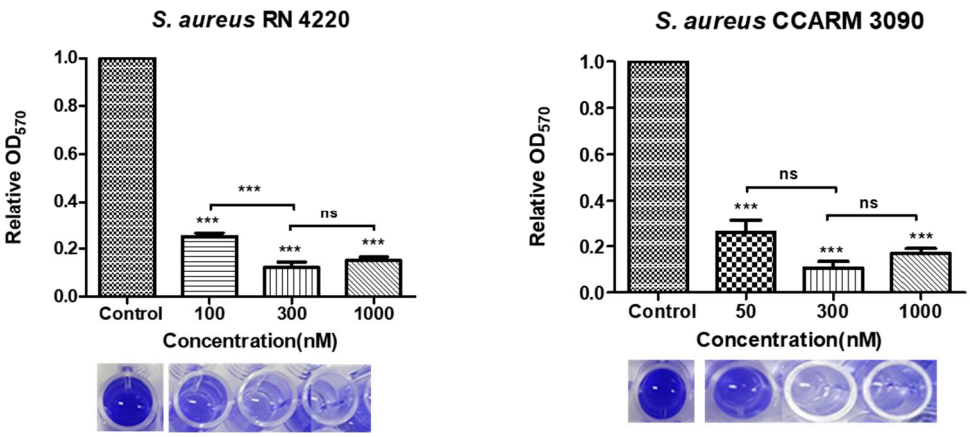

Figure 12. Removal of 24 h-old biofilm on 96-well polystyrene microplate with LysCSA13. Biofilms of *S. aureus* RN4220, and CCARM 3090 were treated with 300 nM of LysCSA13 for 2 h. Each column represents the mean of triplicate experiments, and error bars indicate the standard deviation.

3.6. Biofilm reduction efficacy of LysCSA13 on various contact surfaces

To investigate biofilm reduction efficacy on various contact surfaces, activity of LysCSA13 was additionally tested on stainless steel and glass (Miao et al. 2017b). Biofilm was formed using *S. aureus* RN4200 and *S. aureus* CCARM 3090, which exhibited the highest biofilm reduction capacity on polystyrene surface. When 300 nM or more endolysin was applied to biofilm formed on stainless steel, 84% and 82% of biofilm mass of *S. aureus* RN4200 and *S. aureus* CCARM 3090 was removed, respectively, compared to untreated control (Figure 13A, B). More notable disruption of the biofilm was observed on glass than those on stainless steel, removing 92% and 88% biofilm mass of *S. aureus* RN4200 and *S. aureus* CCARM 3090, respectively (Figure 13C, D). When biofilm was treated for 5 different time period, 30 min was sufficient to remove about 80% of biofilm mass and no further reduction of biofilm mass was observed after 1 h (Figure 14). Results of viable cell count assay have shown that LysCSA13 reduced the number of sessile cells by about 2 and 3 log orders of magnitude on stainless steel and

glass, respectively (Figure 15). These results indicate that 1 h treatment with 300 nM of LysCSA13 is sufficient for removal of biofilm on both stainless steel and glass.

To strengthen these results, biofilm reduction ability of LysCSA13 was further confirmed by SEM analysis. After 24 h incubation, biofilms of both *S. aureus* RN4220 and *S. aureus* CCARM 3090 were highly organized on stainless steel and biofilm of *S. aureus* RN4220 appeared to be rather compact cell aggregates forming firm biofilm matrix than *S. aureus* CCARM 3090 (Figure 16A, C). When 300 nM LysCSA13 was treated for 4 h in biofilms, most cells were removed and fewer cells were remained on the stainless steel surface compared to its control sample (Figure 16B, D). Furthermore, the remaining cells appeared to be embedded in amorphous material, which could be result of cell lysis (González et al. 2017). These results demonstrated that LysCSA13 has strong anti-biofilm activity on stainless steel and glass as well as polystyrene surface.

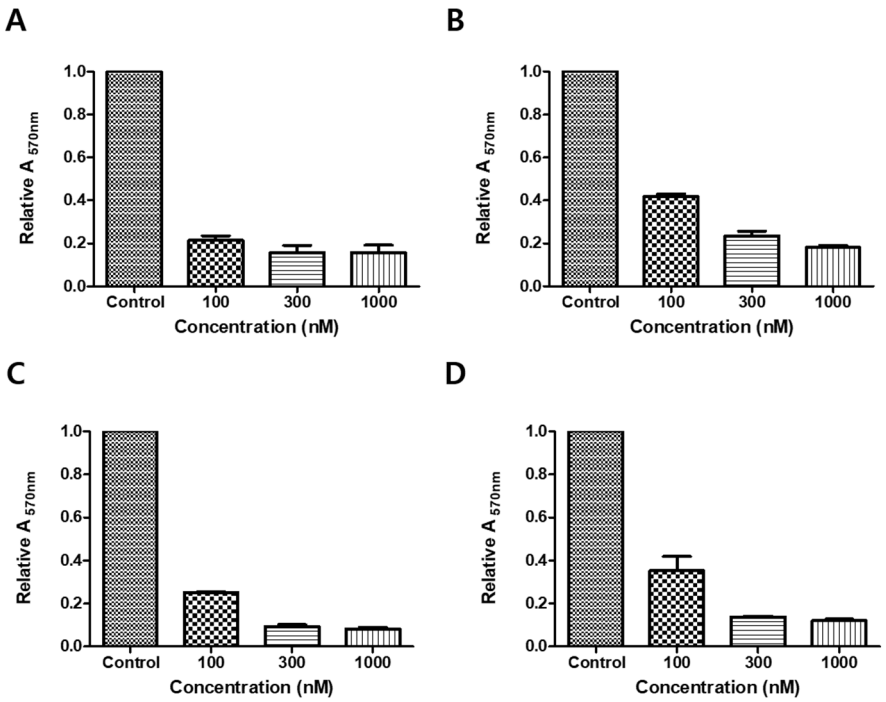

Figure 13. Removal of 24 h-old biofilm on stainless steel and glass with LysCSA13. Biofilms of *S. aureus* RN4220 **(A, C)** and CCARM 3090 **(B, D)** were formed on stainless steel **(A, B)** and glass **(C, D)** treated with three different concentrations of LysCSA13. Biofilm was treated for 1 h for both

of the strains. Each column represents the mean of triplicate experiments, and error bars indicate the standard deviation.

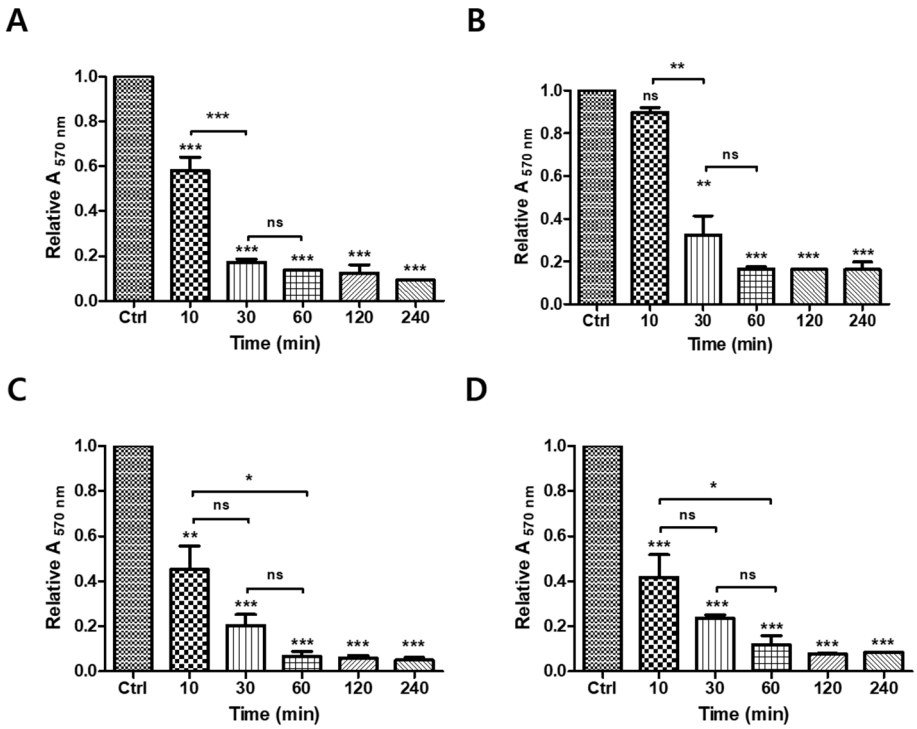

Figure 14. Removal of 24 h-old biofilm for various treatment time with LysCSA13. Biofilms of *S. aureus* RN4220 **(A, C)** and CCARM 3090 **(B, D)** were formed on stainless steel **(A, B)** and glass **(C, D)** with five different treatment time. Each column represents the mean of triplicate experiments,

and error bars indicate the standard deviation. Asterisks indicate significant differences as follows: ***, $P < 0.0001$; **, $P < 0.005$; *, $P < 0.05$. ns, not detected.

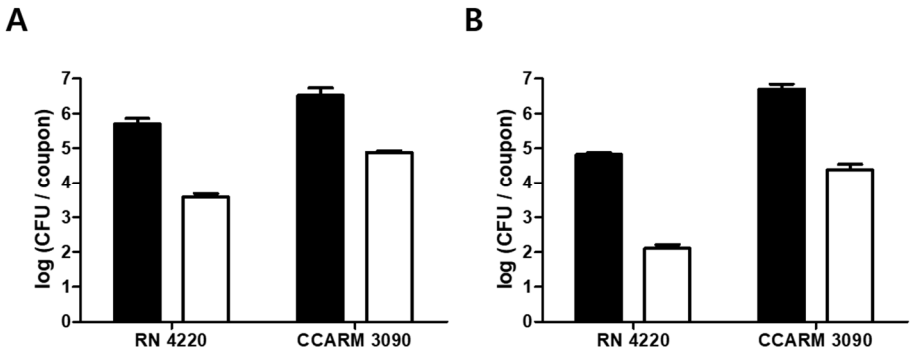

Figure 15.

Viable cell count of 24-h biofilm on various contact surfaces with LysCSA13. 24-h biofilms of *S. aureus* RN4220 and CCARM 3090 were formed on stainless steel **(A)** and glass **(B)**. Biofilm was treated with 300 nM of LysCSA13 (white) for 1 h for both of the strains. Control biofilms are represented in black. Each column represents the mean of triplicate experiments, and error bars indicate the standard deviation.

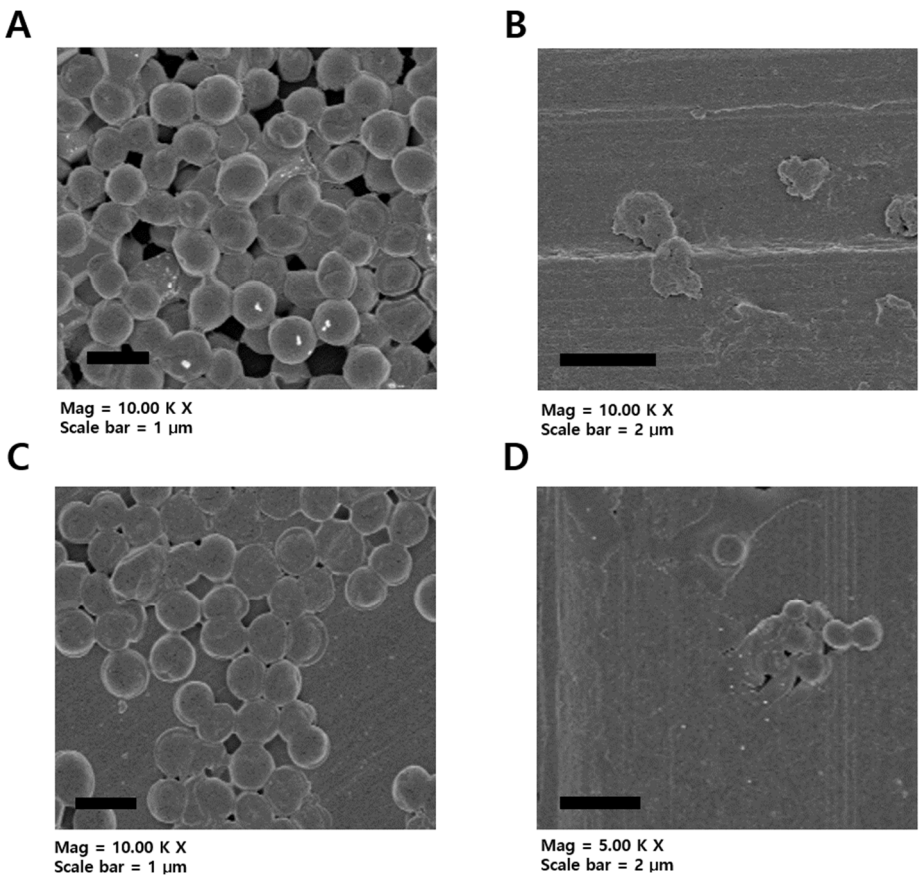

Figure 16. SEM analysis of the degradation of efficacy of LysCSA13 against *S. aureus* RN4220 and CCARM 3090 on stainless steel. Biofilms

formed by *S. aureus* RN4220 **(A, B)** and *S. aureus* CCARM 3090 **(C, D)** was treated with 300 nM of LysCSA13 for 4 h. (*left*, before treatment; *right*, after treatment).

Ⅳ. DISCUSSION

In this study, four bacteriophages targeting *S. aureus* were newly isolated. Among these phages, CSA13 phage possessed broadest host range and most effective inhibition activity. Furthermore, biofilms formed by both *S. aureus* CCARM 3793 and *S. aureus* Newman were successfully removed by phage CSA13 in a PFU-dependent manner. As a result, phage CSA13 was selected for further studies, and we newly identified a gene encoding LysCSA13 endolysin.

LysCSA13 consists of a N-terminal CHAP domain and a C-terminal SH3 domain, and 11% of the reported *S. aureus* endolysins were involved in this domain composition (Chang and Ryu 2017). The optimal lytic activity of LysCSA13 appeared at pH 8.0, a wide range of temperatures and in the absence of NaCl. This enzyme required a divalent metal ion, such as Ca^{2+} and Mn^{2+}, for its full enzymatic activity. However, no Ca^{2+} or Mn^{2+}

coordinating residues were detected through protein sequence analysis. In accordance with this finding, several CHAP domain-containing staphylococcal endolysins have been shown to require Ca^{2+} for their activity (Donovan et al. 2006, Gu et al. 2014, M. et al. 2011). Interestingly, no other endolysin targeting *S. aureus* studied beforehand, showed reactivation of enzymatic activity by Mn^{2+}. However, other endolysins such as *Bacillus colistinus* endolysin CwlV (Shida et al. 2001), bacteriophage T5 endolysin (V. et al. 2009) and *Listeria* phage endolysins HPL118 and HLP511 (Schmelcher et al. 2012) showed effective recovery in enzymatic activity with Mn^{2+}.

LysCSA13 had antimicrobial activity against all tested 15 staphylococcal planktonic cells including MRSA strains. Furthermore, LysCSA13 presented notable disrupting activity against biofilms formed by *S. aureus* including MRSA strains and *S. hominis* strain, showing a 70-90 % reduction in OD_{570} after crystal violet staining compared to a LysCSA13-untreated control. LysCSA13 exhibited maximum 90% decrease in *S. aureus* biofilm when 300 nM (8.51 μg/ml) was treated for 1 h, while other endolysins studied previously had lower biofilm removal efficacy. ClyF showed reduction of 25-50% biofilm mass when 100 μg/ml was treated for 45 min. Another triple-acting fusion protein PGHs presented about 70% decrease of *S. aureus* biofilm when 1400 nM was treated for 2 h. In the case

of the CHAP domain of LysK, about 60% decrease was detected when 15.53 μg/ml was treated for 4 h. We could summarize that LysCSA13 possesses high biofilm removal activity compared to other reported *S. aureus* endolysin.

Beyond the ability of endolysin to remove biofilms, the aim of this study was to remove biofilms on various food contact surfaces. In this regard, we treated LysCSA13 to biofilms formed on stainless steel and glass. Surfaces with high free energy, such as stainless steel and glass, are more hydrophilic and generally allow better attachment of bacteria, leading to biofilm formation at a higher rate in the food processing environments (Chaturongkasumrit et al. 2011). LysCSA13 was effective to reduce up to 93% of mature staphylococcal biofilm mass and to eliminate 3 log of attached bacterial counts within 1 h. There was no significant difference in biofilm reduction efficacy of LysCSA13 between stainless steel and glass in crystal violet assay. However, viable cell count analysis revealed that LysCSA13 more effectively reduce sessile cells of biofilm on glass than those on stainless steel. Generally, biofilms formed on stainless steel are more difficult to be damaged compared to glass, since stainless steel has rough surface resulting stronger cell adhesion (Miao et al. 2017a). This suggest that the effect of biofilm reduction by endolysin might differ depending on the contact surface.

Even though several other *S. aureus* endolysins have recently been developed as introduced above, as far as we know, this study is the first to demonstrate the efficacy of an endolysin to remove biofilms formed on the various food contact surfaces. Our results revealed that LysCSA13 not only control staphylococcal planktonic cells but also effectively control biofilm regardless of contact surfaces including polystyrene, stainless steel and glass. Overall, this study demonstrates the potential use of LysCSA13 as effective anti-biofilm agents in various food processing procedures and environment.

V. REFERENCES

1. Altschul SF, Madden TL, Schäffer AA, Zhang J, Zhang Z, Miller W, Lipman DJ. 1997. Gapped BLAST and PSI-BLAST: a new generation of protein database search programs. Nucleic Acids Research 25:3389-3402.
2. Baba T, Bae T, Schneewind O, Takeuchi F, Hiramatsu K. 2008. Genome sequence of *Staphylococcus aureus* strain Newman and comparative analysis of staphylococcal genomes: polymorphism and evolution of two major pathogenicity islands. J Bacteriol 190:300-310.
3. Besemer J, Lomsadze A, Borodovsky M. 2001. GeneMarkS: a self-training method for prediction of gene starts in microbial genomes. Implications for finding sequence motifs in regulatory regions. Nucleic Acids Research 29:2607-2618.
4. Brückner R. 1992. A series of shuttle vectors for Bacillus subtilis and

Escherichia coli. Gene 122:187-192.

5. Carver TJ, Rutherford KM, Berriman M, Rajandream M-A, Barrell BG, Parkhill J. 2005. ACT: the Artemis Comparison Tool. Bioinformatics (Oxford, England) 21:3422-3423.
6. Chang Y, Lee J-H, Shin H, Heu S, Ryu S. 2013. Characterization and complete genome sequence analysis of *Staphylococcus aureus* bacteriophage SA12. Virus Genes 47:389-393.
7. Chang Y, Ryu S. 2017. Characterization of a novel cell wall binding domain-containing *Staphylococcus aureus* endolysin LysSA97. Applied Microbiology and Biotechnology 101:147-158.
8. Chaturongkasumrit Y, Takahashi H, Keeratipibul S, Kuda T, Kimura B. 2011. The effect of polyesterurethane belt surface roughness on *Listeria monocytogenes* biofilm formation and its cleaning efficiency. Food Control 22:1893-1899.
9. Darling ACE, Mau B, Blattner FR, Perna NT. 2004. Mauve: Multiple Alignment of Conserved Genomic Sequence With Rearrangements. Genome Research 14:1394-1403.
10. Darling AE, Mau B, Perna NT. 2010. progressiveMauve: Multiple Genome Alignment with Gene Gain, Loss and Rearrangement. PLOS ONE 5:e11147.

11. Delcher AL, Bratke KA, Powers EC, Salzberg SL. 2007. Identifying bacterial genes and endosymbiont DNA with Glimmer. Bioinformatics 23:673-679.
12. Donovan DM, Lardeo M, Foster-Frey J. 2006. Lysis of staphylococcal mastitis pathogens by bacteriophage phi11 endolysin. FEMS Microbiology Letters 265:133-139.
13. Dunne M, Mertens HD, Garefalaki V, Jeffries CM, Thompson A, Lemke EA, Svergun DI, Mayer MJ, Narbad A, Meijers R. 2014. The CD27L and CTP1L endolysins targeting *Clostridia* contain a built-in trigger and release factor. PLoS Pathog 10:e1004228.
14. Felsenstein J. 1985. Confidence Limits on Phylogenies: An Approach Using the Bootstrap. Evolution 39:783-791.
15. Fenton M, Keary R, McAuliffe O, Ross RP, O'Mahony J, Coffey A. 2013. Bacteriophage-Derived Peptidase CHAP(K) Eliminates and Prevents Staphylococcal Biofilms. Int J Microbiol 2013:625341.
16. Flemming H-C, Wingender J. 2010. The biofilm matrix. Nature Reviews Microbiology 8:623.
17. Gaeng S, Scherer S, Neve H, Loessner MJ. 2000. Gene Cloning and Expression and Secretion of *Listeria monocytogenes* Bacteriophage-Lytic Enzymes in *Lactococcus lactis*. Applied and Environmental

Microbiology 66:2951-2958.

18. González S, Fernández L, Campelo AB, Gutiérrez D, Martínez B, Rodríguez A, García P. 2017. The Behavior of *Staphylococcus aureus* Dual-Species Biofilms Treated with Bacteriophage phiIPLA-RODI Depends on the Accompanying Microorganism. Applied and Environmental Microbiology 83:e02821-02816.
19. Gu J, et al. 2014. Structural and Biochemical Characterization Reveals LysGH15 as an Unprecedented "EF-Hand-Like" Calcium-Binding Phage Lysin. PLOS Pathogens 10:e1004109.
20. Gutierrez D, Rodriguez-Rubio L, Martinez B, Rodriguez A, Garcia P. 2016. Bacteriophages as Weapons Against Bacterial Biofilms in the Food Industry. Front Microbiol 7:825.
21. Gutierrez D, Ruas-Madiedo P, Martinez B, Rodriguez A, Garcia P. 2014. Effective removal of staphylococcal biofilms by the endolysin LysH5. PLoS One 9:e107307.
22. Jin J-w, Zhang L, Zha X-l, Li H-l, Qu D. 2005. Effect of glucose on biofilm and the gene ica expression in *Staphylococcus epidermidis* with different biofilm-forming capability. Wei sheng wu xue bao = Acta microbiologica Sinica 45:431-436.
23. Kelly D, McAuliffe O, Ross RP, Coffey A. 2012. Prevention of

Staphylococcus aureus biofilm formation and reduction in established biofilm density using a combination of phage K and modified derivatives. Lett Appl Microbiol 54:286-291.

24. Kumar S, Stecher G, Tamura K. 2016. MEGA7: Molecular Evolutionary Genetics Analysis Version 7.0 for Bigger Datasets. Molecular Biology and Evolution 33:1870-1874.
25. Kwiatek M, Parasion S, Mizak L, Gryko R, Bartoszcze M, Kocik J. 2012. Characterization of a bacteriophage, isolated from a cow with mastitis, that is lytic against *Staphylococcus aureus* strains. Archives of Virology 157:225-234.
26. Larkin MA, et al. 2007. Clustal W and Clustal X version 2.0. Bioinformatics 23:2947-2948.
27. Lewis K. 2008. Multidrug Tolerance of Biofilms and Persister Cells.
28. Li X-H, Lee J-H. 2017. Antibiofilm agents: A new perspective for antimicrobial strategy. Journal of Microbiology 55:753-766.
29. Lu Z, Breidt F, Fleming HP, Altermann E, Klaenhammer TR. 2003. Isolation and characterization of a Lactobacillus plantarum bacteriophage, ΦJL-1, from a cucumber fermentation. International Journal of Food Microbiology 84:225-235.
30. M. F, R.P. R, O. M, J. OM, A. C. 2011. Characterization of the

staphylococcal bacteriophage lysin CHAPK. Journal of Applied Microbiology 111:1025-1035.

31. Marques SC, Rezende JdGOS, Alves LAdF, Silva BC, Alves E, Abreu LRd, Piccoli RH. 2007. Formation of biofilms by *Staphylococcus aureus* on stainless steel and glass surfaces and its resistance to some selected chemical sanitizers. v. vol.38 num.3.
32. Miao J, Liang Y, Chen L, Wang W, Wang J, Li B, Li L, Chen D, Xu Z. 2017a. Formation and development of *Staphylococcus* biofilm: With focus on food safety. Journal of Food Safety 37:e12358.
33. Moreira JMR, Gomes LC, Araújo JDP, Miranda JM, Simões M, Melo LF, Mergulhão FJ. 2013. The effect of glucose concentration and shaking conditions on *Escherichia coli* biofilm formation in microtiter plates. Chemical Engineering Science 94:192-199.
34. Nei M, Kumar S. 2000. Molecular evolution and phylogenetics. Oxford university press.
35. Oku Y, Kurokawa K, Matsuo M, Yamada S, Lee B-L, Sekimizu K. 2009. Pleiotropic Roles of Polyglycerolphosphate Synthase of Lipoteichoic Acid in Growth of *Staphylococcus aureus* Cells. Journal of Bacteriology 191:141.
36. Park K-H, et al. 2010a. Human serum mannose-binding lectin senses

wall teichoic acid Glycopolymer of *Staphylococcus aureus*, which is restricted in infancy. The Journal of biological chemistry 285:27167-27175.

37. Park KH, et al. 2010b. Human serum mannose-binding lectin senses wall teichoic acid Glycopolymer of *Staphylococcus aureus*, which is restricted in infancy. J Biol Chem 285:27167-27175.
38. Park M, Lee JH, Shin H, Kim M, Choi J, Kang DH, Heu S, Ryu S. 2012. Characterization and comparative genomic analysis of a novel bacteriophage, SFP10, simultaneously inhibiting both Salmonella enterica and Escherichia coli O157:H7. Appl Environ Microbiol 78:58-69.
39. Saitou N, Nei M. 1987. The neighbor-joining method: a new method for reconstructing phylogenetic trees. Molecular Biology and Evolution 4:406-425.
40. Schleifer KH, Kandler O. 1972. Peptidoglycan types of bacterial cell walls and their taxonomic implications. Bacteriological Reviews 36:407-477.
41. Schmelcher M, Waldherr F, Loessner MJ. 2012. *Listeria* bacteriophage peptidoglycan hydrolases feature high thermoresistance and reveal increased activity after divalent metal cation substitution. Applied

Microbiology and Biotechnology 93:633-643.

42. Sharma U, Vipra A, Channabasappa S. 2018. Phage-derived lysins as potential agents for eradicating biofilms and persisters. Drug Discovery Today 23:848-856.

43. Shida T, Hattori H, Ise F, Sekiguchi J. 2001. Mutational analysis of catalytic sites of the cell wall lytic N-acetylmuramoyl-L-alanine amidases CwlC and CwlV. J Biol Chem 276:28140-28146.

44. Sillankorva S, Neubauer P, Azeredo J. 2008. *Pseudomonas* fluorescens biofilms subjected to phage phiIBB-PF7A. BMC Biotechnology 8:79.

45. Son B, Yun J, Lim J-A, Shin H, Heu S, Ryu S. 2012. Characterization of LysB4, an endolysin from the *Bacillus cereus*-infecting bacteriophage B4. BMC Microbiology 12:33.

46. Son J-S, Lee S-J, Jun SY, Yoon SJ, Kang SH, Paik HR, Kang JO, Choi Y-J. 2010a. Antibacterial and biofilm removal activity of a podoviridae *Staphylococcus aureus* bacteriophage SAP-2 and a derived recombinant cell-wall-degrading enzyme. Applied Microbiology and Biotechnology 86:1439-1449.

47. Son JS, Lee SJ, Jun SY, Yoon SJ, Kang SH, Paik HR, Kang JO, Choi YJ. 2010b. Antibacterial and biofilm removal activity of a podoviridae *Staphylococcus aureus* bacteriophage SAP-2 and a derived recombinant

cell-wall-degrading enzyme. Appl Microbiol Biotechnol 86:1439-1449.

48. Stewart PS. 2002. Mechanisms of antibiotic resistance in bacterial biofilms. Int J Med Microbiol 292:107-113.
49. Swoboda JG, Campbell J, Meredith TC, Walker S. 2010. Wall teichoic acid function, biosynthesis, and inhibition. Chembiochem : a European journal of chemical biology 11:35-45.
50. Thompson JD, Higgins DG, Gibson TJ. 1994. CLUSTAL W: improving the sensitivity of progressive multiple sequence alignment through sequence weighting, position-specific gap penalties and weight matrix choice. Nucleic Acids Research 22:4673-4680.
51. V. MG, V. OI, A. ZA, Ya. LV, A. FS, A. SO. 2009. Identification and characterization of the metal ion-dependent l-alanoyl-d-glutamate peptidase encoded by bacteriophage T5. The FEBS Journal 276:7329-7342.
52. Vybiral D, TakÃ¡Ä M, Loessner M, Witte A, Ahsen U, BlÃ¤si U. 2003. Complete nucleotide sequence and molecular characterization of two lytic *Staphylococcus aureus* phages: 44AHJD and P68. FEMS Microbiology Letters 219:275-283.
53. Wann ER, Dassy B, Fournier J-M, Foster TJ. 2006. Genetic analysis of the cap5 locus of *Staphylococcus aureus*. FEMS Microbiology Letters

170:97-103.

54. Wilcox SA, Toder R, Foster JW. 1996. Rapid isolation of recombinant lambda phage DNA for use in fluorescence in situ hybridization. Chromosome Research 4:397-404.

55. Wu JA, Kusuma C, Mond JJ, Kokai-Kun JF. 2003. Lysostaphin Disrupts *Staphylococcus aureus* and *Staphylococcus epidermidis* Biofilms on Artificial Surfaces. Antimicrobial Agents and Chemotherapy 47:3407-3414.

56. Xia G, Corrigan RM, Winstel V, Goerke C, Gründling A, Peschel A. 2011. Wall Teichoic Acid-Dependent Adsorption of Staphylococcal Siphovirus and Myovirus. Journal of Bacteriology 193:4006.

57. Žiedaitė G, Daugelavičius R, Bamford JKH, Bamford DH. 2005. The Holin Protein of Bacteriophage PRD1 Forms a Pore for Small-Molecule and Endolysin Translocation. Journal of Bacteriology 187:5397.

국문 초록

황색포도상구균 (*Staphylococcus aureus*)은 화농성 피부염, 심장 내막염, 폐혈증 및 독성 쇼크 증후군 등 생명을 위협하는 질병을 유발하는 병원균이다. 임상 환경에서 메티실린 및 반코마이신 저항성 황색포도상구균과 같은 항생제 내성 균주의 출현은 전세계적으로 심각한 위협을 제기한다. 더 나아가, 세포의 폴리머에 의해 고체 표면에 부착하여 균집합체인 생물막을 형성한다. 생물막은 기존의 항생제 및 기타 환경적 스트레스에 강하다는 특징을 지니므로, 식품 및 의료 산업에서 중요한 문제로

인식된다. 이에 따라, 기존의 항생제를 대체하기 위한 생물제제로 박테리오파지 및 파지에서 분리된 세포벽 분해 효소인 엔돌라이신이 각광받고 있다. 본 연구에서는, 황색포도상구균에 특이적으로 감염할 수 있는 포도비리데 과에 속하는 파지 CSA13을 닭에서 분리하고, 이에 대한 특성 분석을 시행하였다. CSA13은 23 시간 동안 지속적으로 황색포도상구균 숙주의 증식을 억제하였으며, MRSA를 포함한 10 종의 포도상구균과 15 종의 임상 분리 균을 효과적으로 감염했으며, 3 종의 다른 포도상구균에도 사멸능을 보였다. 더 나아가, MSSA 및 MRSA 생물막의 78 % 및 93 % 이상을 성공적으로 제거하였다. 유전체 분석 결과, CSA13 유전체는 17,034 bp 길이의 이중나선 DNA로 구성되며, 18개의 ORF가 예측되었으며 tRNA는 존재하지 않았다. 18개의 예측된 유전자 중 N-acetyl-muramoyl-L-alanine amidase와 상동성이 높은 엔돌라이신 유전자가 확인되었다. LysCSA13은 효소적 활성을 나타내는 도메인인 CHAP, 그리고 세포 부착 기능을 수행하는 도메인인 SH3로 구성되어 있는 것을 확인하였다. LysCSA13은 pH 8.0과 25 ℃에서 최적의 효소 활성을 나타냈으며, 검사한 모든 15

종의 포도상구균에 대하여 강한 항균 활성을 보였다. 또한 폴리스티렌, 유리 및 스테인리스에 형성된 포도상구균 생물막의 80-90 % 감소 효과를 보였다. 유리와 스테인리스에서 엔돌라이신이 처리되지 않은 대조군에 비해 1-3 로그의 포도상구균을 제거하였으며, 주사전자현미경을 통하여 생물막 매트릭스에 박혀있는 세포의 변형과 제거를 시각적으로 확인하였다.

주요어: 황색포도상구균, 박테리오파지, 엔도라이신, 바이오필름

학번: 2017-23691